

First Principles studies of band structure and electronic properties of Group III – Nitrides Semiconductors

O. D. Ojuh ^{1,2} and J. O. A Idiodi ¹.

1. Physics Department, University of Benin, Benin City, Nigeria.
2. Department of Basic Sciences, Benson Idahosa University, Benin City Nigeria.

Abstract

The electronic properties of group III – Nitrides semiconductor are investigated by performing first principles calculations using Density Functional Theory (DFT). The exchange correlation potentials were treated within the Local Density Approximation (LDA) and the Generalized Gradient Approximation (GGA) with the Abinit (Pseudopotential) and Bandlab (Full Potential Linear Muffin-Tin Orbital) have been used to investigate the electronic band structure. From these band structures, the necessary band gaps have been deduced. The present calculations have shown direct band gap energy in the zincblende phase for AlN, InN, GaN, and indirect band gap energy for BN. Here, the conduction band minima of AlN, InN and GaN are located at Γ -point, while that of BN is at a position lying along the Γ -X direction of the Brillouin zone.

1.0 INTRODUCTION

In the last few years no other class of semiconductors has attracted so much scientific and commercial attention like the group III - nitrides (AlN, BN, GaN and InN). The increasing interest is due to their extraordinary physical properties, which have been found to be useful in many new electronic and optoelectronic devices. The development of group-III nitrides in the late 1990's has been motivated by the realization of efficient light emitting diodes (LED), which are now an industrial standard for solid state lighting [1,2]. Other significant applications of group-III nitrides are high-frequency/high-power electronics using high-electron-mobility transistors (HEMT) and photodetectors [3,4]. Photodetectors based on group-III nitrides take advantage of their inherent spectral selectivity to allow for the tuning of the detection edge from about 200 nm (AlN) to about 1770 nm (InN). Some potential benefits added by the use of these materials are their radiation hardness and the expected lower intrinsic noise and dark current in comparison with narrow-band-gap materials (e.g., Si) [5, 6]. In addition, the devised applications comprise, for example, solar-blind detection [7,8], non-line-of-sight ultraviolet (UV) communications [9], combustion monitoring [10], space communications [11], high-resolution photolithography together with emitters [and missile plume detection [11]. Similarly, solar cells fabricated with (In,Ga)N compounds operating in the 2.4 eV range, as photodetectorlike devices, are a promising technology to increase the conversion efficiency of current photovoltaic cells [12-13]. The increasing commercial attention has equally led to increasing theoretical interest. However, theoretical band structure calculations of the binary compounds AlN, BN, GaN and InN in the zincblende structure have failed to predict the band gaps experimentally observed in them.

In this work, the Pseudopotential and Full Potential Linear Muffin-Tin Orbital method (FP-LMTO) in the Density functional theory (DFT) of the Local density approximation (LDA) and generalized gradient approximation (GGA) have been used to investigate the electronic band structure of binary compounds AlN, BN, GaN and InN in zincblende structure. From these band structures, the necessary band gaps have been deduced. The band structure calculations have been implemented with two computer codes, namely, Abinit (Pseudopotential) and Bandlab (Full Potential Linear Muffin-Tin Orbital).

2.0 METHOD OF CALCULATION

2.1 Total Energy and Functional

Solving the many-body Schrödinger equation allows to obtain many properties of a system of N interacting electrons in the external potential of the nuclei. The Hamiltonian equation is given as:

$$H\psi(r_1, \dots, r_{N_{el}}) = E\psi(r_1, \dots, r_{N_{el}}) \quad 2.1.1$$

While the Schrödinger is state below:

$$H = -\sum_i \hbar^2 / 2M\Delta_i^2 + \sum_i V_{ext}(r_i) + e^2 / 2\sum_{i \neq j} 1 / |r_i - r_j| \quad 2.1.2$$

Where r_i is the position of electron i , Δ_i^2 indicates the Laplacian taken with respect to the coordinate r_i , while $V_{ext}(r_i)$ is the external potential acting on the electrons and depends parametrically on the nuclear positions. In finding a numerical solution for the Schrödinger equation (2.1.1), an efficient method is required. Density Functional Theory (DFT) introduced by Hohenberg and Kohn [14] provides a one-to-one correspondence between the ground-state electronic charge density $\rho(r)$ and the external potential $V_{ext}(r)$. Therefore, since the external potential determines also the many-body wave-function of the ground state, every physical quantity of the system in its ground state can be expressed as a functional of the electronic charge density. The ground-state total energy of the system plays a prominent role in determining properties of a system, this can be expressed as the expectation value of the Hamiltonian on the ground-state wave-function Ψ_0 . If we express the total energy as a functional of the electronic density then [14, 15],

$$E[\rho(r)] = \langle \Psi_0 | H | \Psi_0 \rangle = F[\rho(r)] + \int_V V_{ext}(r)\rho(r) d^3 r \quad 2.13$$

Where the integral is performed over the whole volume V of the system. In this equation (2.1.3), $F[\rho(r)]$ is a universal functional of the density and it is given by the expectation value of the kinetic energy and of electrostatic electron repulsion terms on the ground state. The minimization of the functional $E[\rho(r)]$ with respect to the electronic density, with the constraint that the number of electrons N_{el} is fixed,

$$\int_V \rho(r) d^3 r = N_{el} \quad 2.1.4$$

Gives the ground-state total energy and the electronic density. Kohn and Sham (KS) [15] introduced a new functional by mapping the many-body problem into a non-interacting electrons problem with the same ground-state electronic density because, the exact form of the universal functional $F[\rho(r)]$ is not known. The new functional can be obtained by recasting the second term in eq. (2.1.3) to the form [14,15]:

$$F[\rho(r)] = T_0[\rho(r)] + E_H + E_{XC}[\rho(r)] \quad 2.1.5$$

Where the first term is the kinetic energy of a non-interacting electrons system, the second term is the Hartree-like energy term, which accounts for the classical Coulomb interaction of a spatial charge distribution $\rho(r)$ and the third term represents the exchange-correlation energy [14,15]. The only really unknown quantity is the exchange-correlation energy functional and, in principle, the quality of the solution of the full many-body problem will be only limited by the quality of the approximation. With this new expression for the functional then, the total energy in eq. (2.1.3) becomes:

$$E[\rho(r)] = \langle \Psi_0 | H | \Psi_0 \rangle = T_0[\rho(r)] + E_H + E_{XC}[\rho(r)] + \int_V V_{ext}(r)\rho(r) d^3 r \quad 2.16$$

In order to account for the exchange-correlation energy functional in the above equation, we applied a Local Density Approximation (LDA) and Generalized Gradient Approximation (GGA) [14,15].

2.2 First-principles methods

In this work, all calculations were done using the Pseudopotential method as implemented by Abinit code[16-18] (which is based on the density functional theory in the local density approximation and generalized gradient approximation is used) and also the full potential-linear muffin-tin orbital (FP-LMTO) method as implemented in the Bandlab code[19,20]. Bloch wave functions of electrons are expanded in terms of plane waves with a cut-off energy of 60 Hartree, and are sampled on an $8 \times 8 \times 8$ grid of k-points in the first Brillouin zone. We use different choices of exchange correlation energy functionals. For LDA calculations, we use the one parametrized by Teter [21] along with Teter's extended norm-conserving pseudopotentials [22]. For GGA calculations, we use "PBE" [23]

The band structure of the binary compounds (AlN, BN, GaN and InN) were obtained. The zincblende structure of the binary compounds (AlN, BN, GaN and InN) is characterized by the lattice constant, a . In this work the experimental lattice constants used are shown in Table 1.

3.0 RESULTS AND DISCUSSION

Figures 3.1 to 3.16 show the calculated band structures. The energy band gap for AlN is found to be (3.341 and 3.208) eV for LMTO and ABINIT respectively, using LDA method, and (3.3986 and 3.261) eV respectively, using GGA method.

We notice that the ZB-AlN is indirect band gap from the Γ point, at the X point for the ABINIT code while the ZB-AlN is direct band gap at the Γ point for the FP-LMTO. Comparing LDA and GGA calculations in the ZB-AlN we see that the band structures are similar, except that the band gap at Γ point for the LDA is smaller than the GGA results. Furthermore, the band structure from ABINIT code is in close agreement with the FP-LAPW results of previous reports of [24, 25].

The Figures 3.5 - 3.5 showed the result of band structure calculations of GaN from Abinit (LDA) and Bandlab (LDA and GGA) respectively, plotted along line of high symmetry. GaN has a direct band gap at the Γ - point, that is the valence maximum and the conduction minimum are at Γ . The value of the calculated band gap is found to be 2.625 eV, 3.577 eV and 1.3207 and 1.7733 eV for Abinit(LDA) and Bandlab(LDA and GGA) respectively. Previously, [26] in their calculation obtained a band gap of 2.3 eV and 3.5 eV for LDA and GW respectively. Zhao et al [27] in their LDA BZW calculation observed a band gap of 3.2 eV, The experimental value is 3.5 eV [28]

It can be seen from Figures 3.7 and 3.8 that the results from the calculations from Bandlab (LDA and GGA) and that of [29] are in qualitative agreement (i.e the shapes of the band structure compared are the same). Also, Figures 3.5 and 3.6 show that the present results are in good agreement with [26] in their calculation, where they obtained a band gap of 2.3 eV and 3.5 eV for LDA and GW.

Figures 3.9 - 3.12 show the energy band gap for ZB-BN. It is found to be 4.21eV and 4.49 eV for Abinit (LDA and GGA) methods respectively while the LMTO (LDA and GGA) methods give 4.843 eV and 4.80eV. We notice that the energy band gap for ZB-BN is indirect (Γ -X). The energy band gap for ZB -BN in GGA method is in close agreement with other calculations. The conduction bands in LDA calculations are shifted a little down with respect to those of the GGA which is leading to a reduction of the band within the ZB-BN structure. As it is observed in Fig. 3.9 and 3.10, the valence band structure of c-BN by DFT-GGA and DFT-LDA from Abinit code gave approximately the similar result which was obtained using DFT/FP-LAPW-(GGA) [24,30] and the Bandlab FP-LMTO (GGA and LDA) 4.803 and 4.843eV of c-BN is slightly greater than the previously reported values of

orthogonalized-plane wave OPW and plane-wave-gaussian PWG [30]. The present DFT calculations within GGA do not give any new feature on the band structure of DFT-LDA. This is an accepted result that the DFT-GGA electronic band structure are qualitatively in good agreement with the experiments in what concerns the energy levels and the shape of the bands.

In table 2, we notice that the energy band gap for InN compound is small. The energy band gap for InN compound in LDA and GGA calculations seem to be in a good agreement compared to the other calculations. The ABINIT and LMTO methods within the Frame work of the DFT-LDA and GGA has been employed to calculate the band structure of InN. It is found that, the band gap of InN is direct in zincblende phase, furthermore, the energy bands is in agreement with the results of previous reports by Stampfi and Van de Walle [30] The present band edge at Γ point is non parabolic as it was reported in these works. Since we are unaware of reports of experimental investigations of the electronic properties of c-InN, we could not compare the present band gap values with the experimental results. But, the present band gap at point E_g^{Γ} is found to be close -0.516 eV with respect to the values -0.48 eV it is only 6.98% smaller than the above magnitude given by ETB [31]. The similar negative and positive direct band gap energies were reported before in the literature.

The energy band gap for InN compound in LDA calculation is overestimated than the energy band gap in GGA calculation. Figures 3.13 - 3.16 show the calculated band structure of InN from Abinit (LDA and GGA) and LMTO respectively.

Table 1: *Lattice constants adopted in this work.*

Compound	Lattice (nm) a
BN	0.369[31]
AlN	0.437[32]
GaN	0.450[31]
InN	0.498[33]

Table 2.0: *A summary of energy gap (p. Cal) compared to other theoretical calculations and experimental results.*

METHOD		AlN		GaN		BN		InN	
		P. Cal	Th/Ex	P. Cal	Th/Ex	P. Cal	Th/Ex	P. Cal	Th/Ex
ABINIT	LDA	3.208	2.700 ^a 3.200 ^b	2.630	1.490 ⁱ 1.800 ^f	4.210	4.200 ^k 4.430 ^{a-k}	-0.389	-0.200 ⁿ -0.400 ⁿ
	GGA	3.261	3.270 ^a 3.300 ^b	2.920	3.500^o 2.000 ^r 1.720 ^q	4.490	4.350 ^a 4.450 ⁱ 6.000 ^k	0.000	-0.550 ⁿ -0.480 ^m -0.517 ^m
LMTO	LDA	3.341	6.300^c 5.940^c 4.940 ^d 4.500 ^d	1.820	2.300 ^o 3.200 ^p	4.800	7.200ⁱ 6.400 ^k	-0.406	
	GGA	3.399		1.770		4.840		-0.180	

^a[24], ^b[25], ^c[38][39]^d[34], ^e[40]f[29]g[28]k[36] l[30], ^m[31]ⁿ[37] ^o[26] ^p[35]

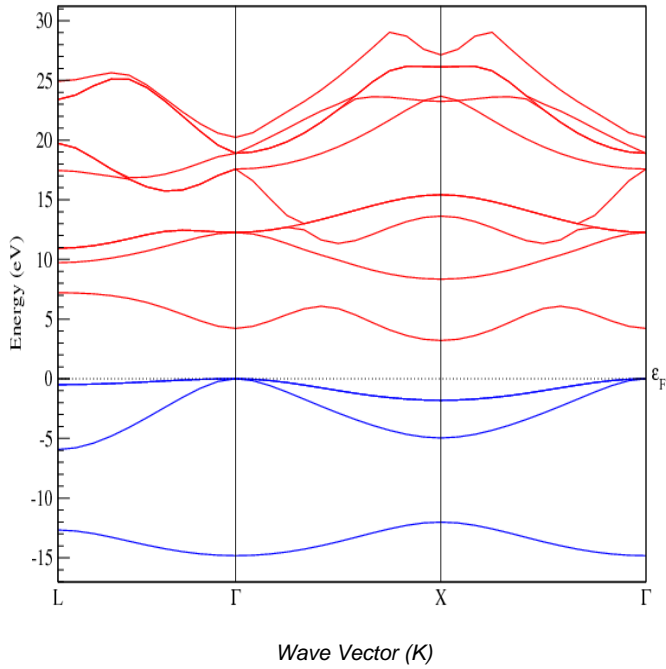


Fig.3.1: The band structure of AlN from ABINIT (LDA). Indirect Band gap is 3.208eV

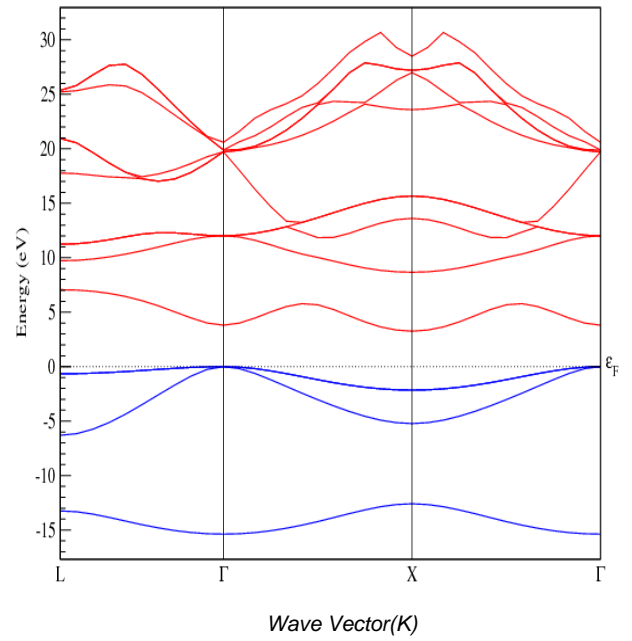


Fig.3.2: The band structure of AlN from ABINIT (GGA). Indirect Band gap is 3.261eV

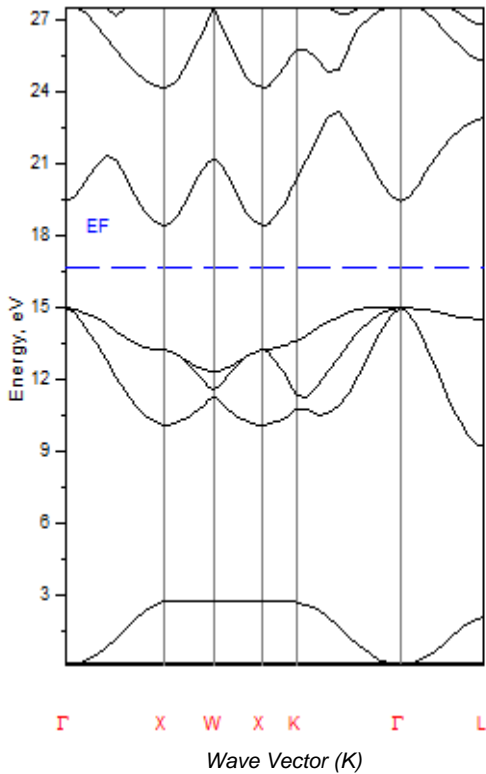


Fig.3.3: The band structure of AlN from Bandlab (LDA). Indirect Band gap is 3.314eV

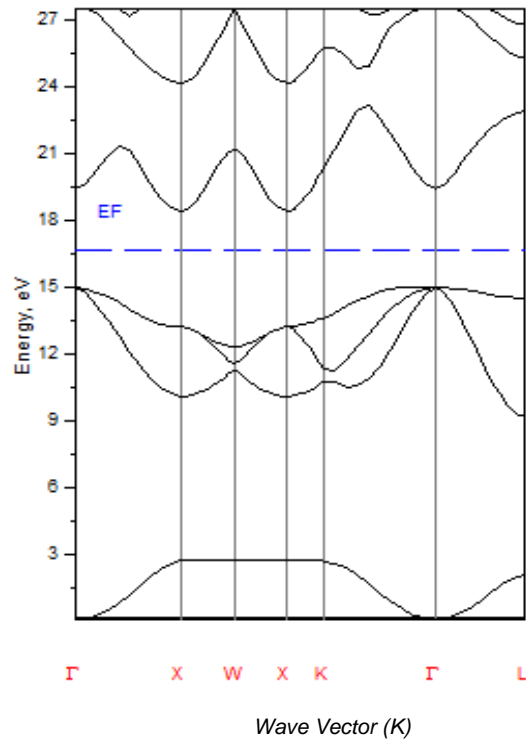
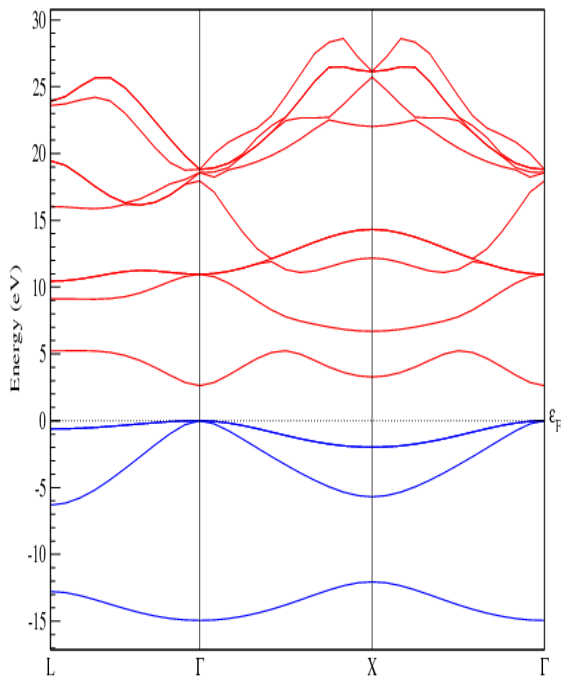
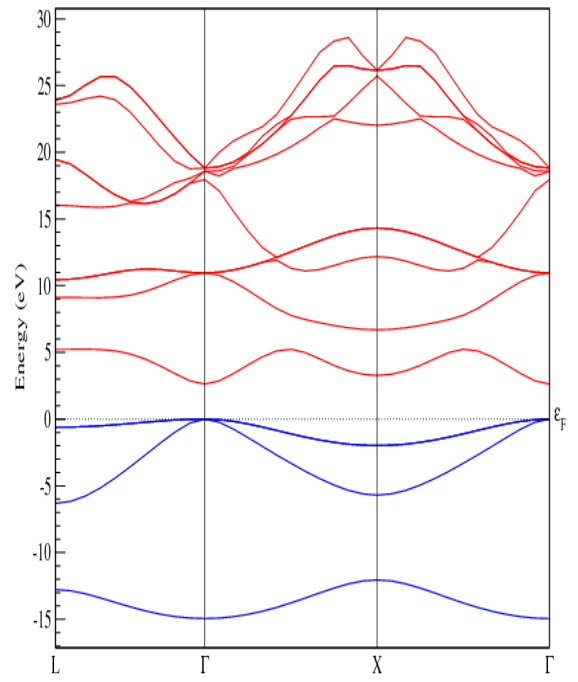


Fig.3.4: The band structure of AlN from Bandlab (GGA). Indirect Band gap is 3.398eV



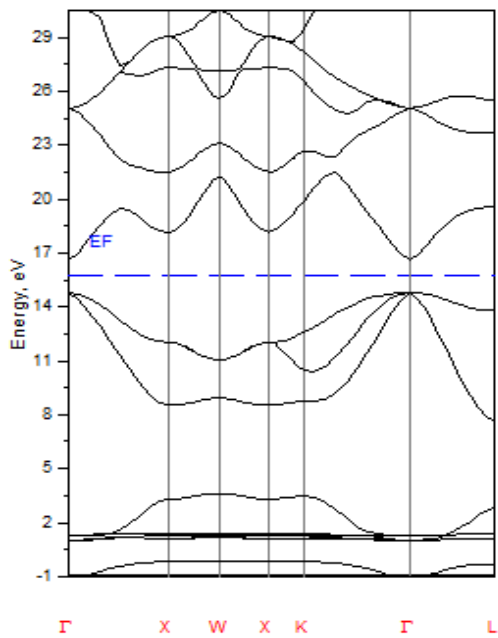
Wave Vector(K)

Fig.3.5: The band structure of GaN from Abinit (LDA).
Direct Band gap is 2.6250eV



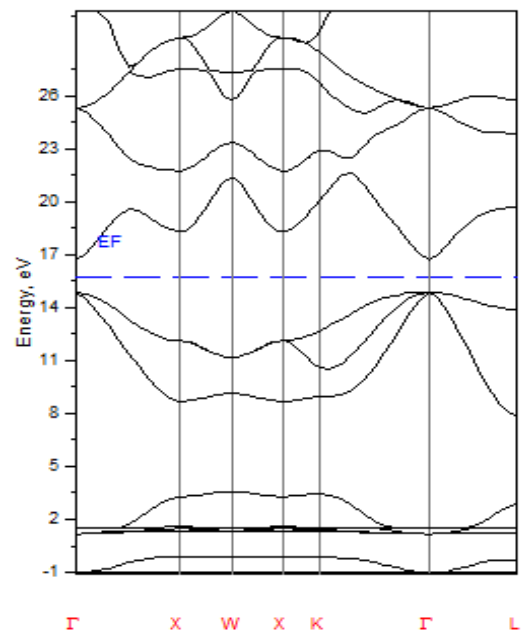
Wave Vector(K)

Fig.3.6: The band structure of GaN from Abinit (GGA). Direct Band gap is 3.398eV



Wave Vector(K)

Fig.3.7: The band structure of GaN from Bandlab(LDA). Direct Band gap is 1.821eV.



Wave Vector(K)

Fig.3.8: The band structure of GaN from Bandlab(LDA). Direct Band gap is 1.773eV.

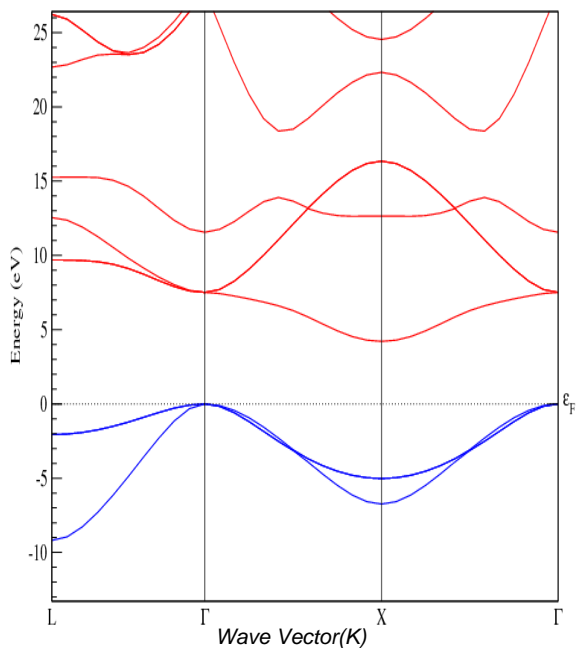


Fig.3.9: The band structure of BN from Abinit (LDA).
Indirect Band gap is 4.21 eV.

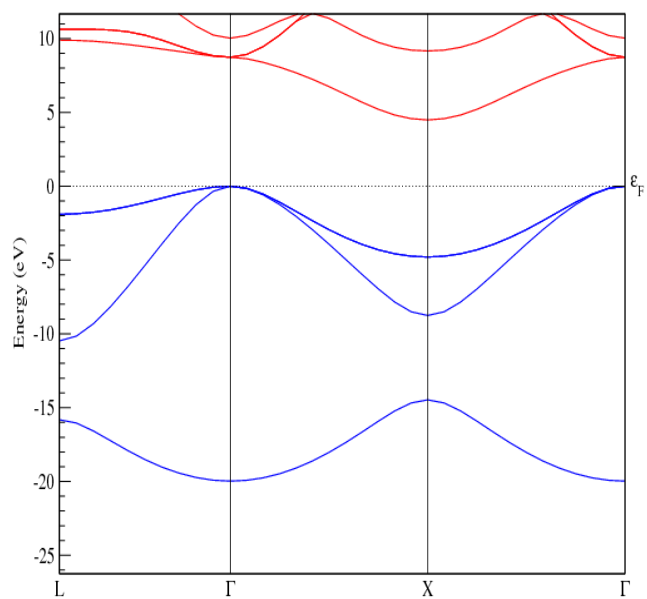


Fig.3.10 The band structure of BN from Abinit (GGA).
Direct Band gap is 4.49 eV.

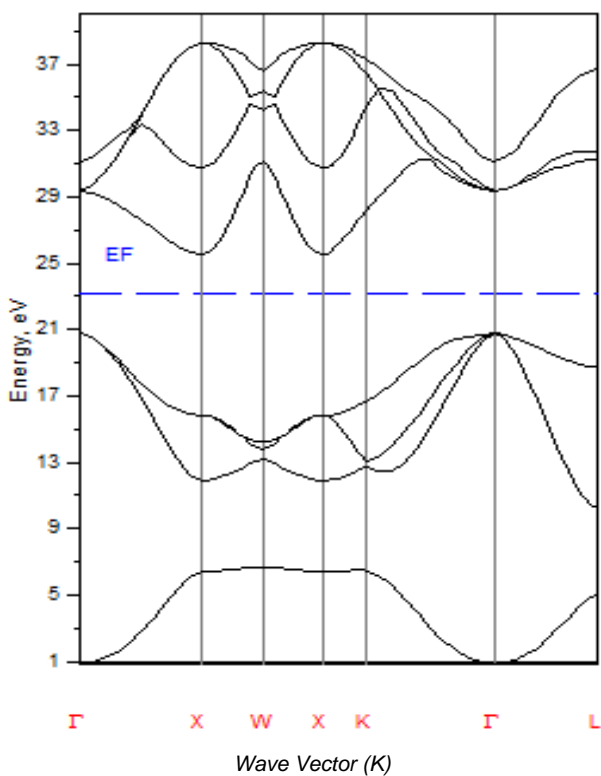


Fig.3.11: The band structure of BN from Bandlab (LDA). Indirect Band gap is 4.803 eV.

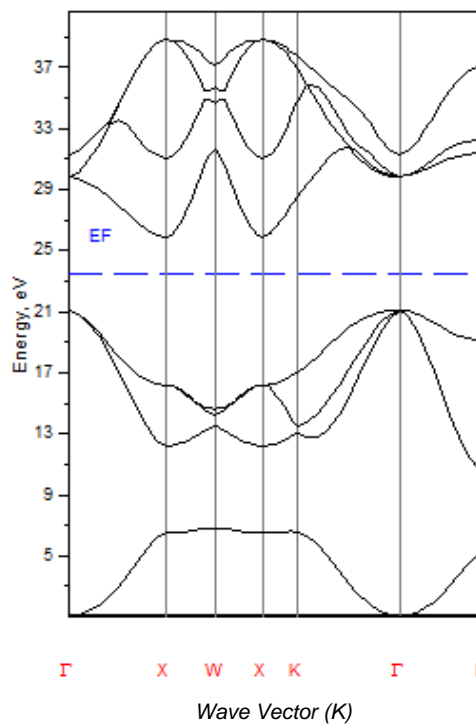


Fig.3.12: The band structure of BN from Bandlab (GGA). Indirect Band gap is 4.843 eV.

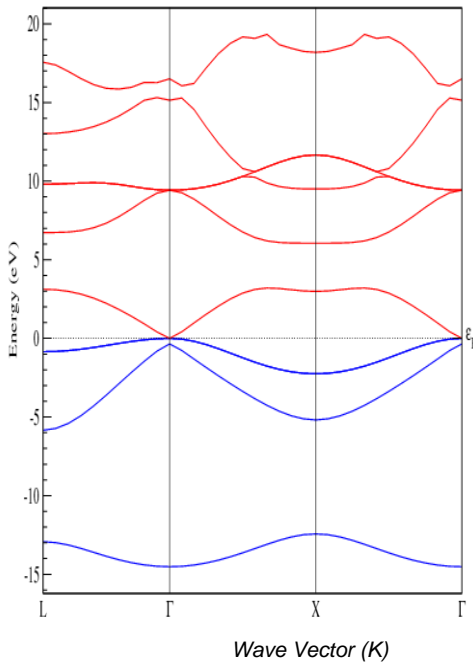


Fig.3.13: The band structure of InN from Abinit (LDA). Direct Band gap is -0.389 eV.

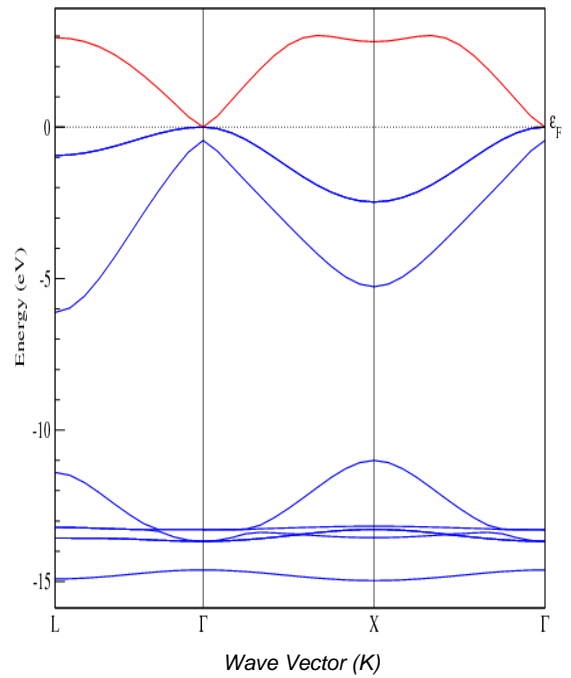


Fig.3.14: The band structure of BN from Bandlab (GGA). Direct Band gap is 0.000 eV.

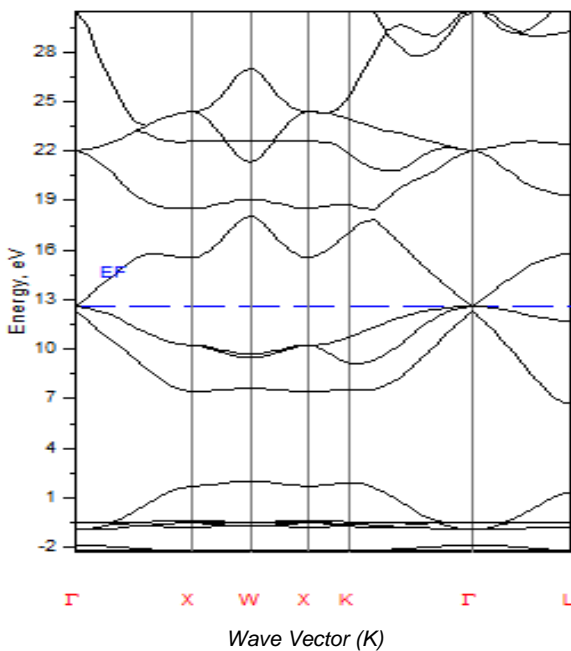


Fig.3.15: The band structure of InN from Bandlab (LDA). Direct Band gap is -0.406 eV.

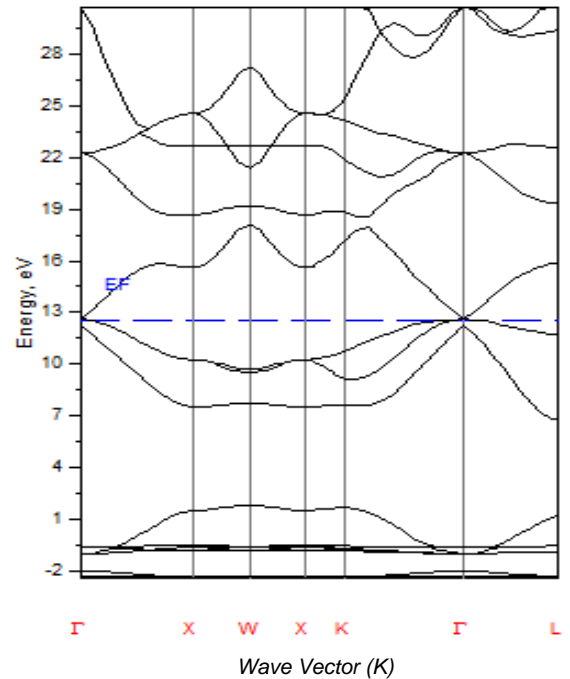


Fig.3.16: The band structure of InN from Bandlab (GGA). Direct Band gap is -0.187 eV.

4.0 CONCLUSION

The results from Abinit code and LMTO, in this study, predicted AlN under LDA and GGA calculations, in this study, predicted AlN to be a semiconductor with a band gap ranging from 3.20 – 3.40eV. While this disagrees with the experimental band gap value, the band gap range is in agreement with the theoretical results of [24, 25, and 34].

The results from LMTO and Abinit codes predicted GaN to be a semiconductor with a band gap ranging from 1.77 – 3.57eV. This is in agreement with both experimental result [28] and theoretical results of [26, 29,31,35]. The results from LMTO and the Abinit code under LDA and GGA calculations predicted BN to be a semiconductor with a band gap ranging

from 4.02 – 4.80eV. While this disagrees with the experimental band gap value, the band gap range is in agreement with the theoretical results of [24,30, 36].

The results from LMTO and Abinit codes under LDA and GGA calculation predicted InN to be a semimetal with a band gap ranging from -0.41 – 0.38eV. This is in agreement with the theoretical results of [24, 30, 31, and 37].

The calculations have shown direct band gap energy for InN, GaN, and indirect band gap energy for AlN and BN in the Abinit code. This is in agreement with the theoretical results of [24, 37]. While AlN, InN and GaN are predicted to be direct band gap materials, BN is predicted to be indirect under the LMTO code in agreement with the theoretical results of [30, 31].

REFERENCES

- [1]. S. Nakamura, and G. Fasol, *The Blue Laser Diode*. Berlin, Springer, 1997.
- [2]. C. Wetzel, M. Zhu, J. Senawiratne, T. Detchprohm, P.D. Persans, L. Liu, E.A. Preble, and D. Hanser, "Light-emitting diode development on polar and non-polar GaN substrates", *J. Cryst. Growth*, vol. 310, pp. 3987-3991, 2008.
- [3]. U.K. Mishra, L. Shen, T.E. Kazior, and Y.F. Wu, "GaN-Based RF Power Devices and Amplifiers", *Proc. IEEE*, vol. 96, pp. 287-305, 2008.
- [4]. E. Muñoz, E. Monroy, J.L. Pau, F. Calle, F. Omnès, and P. Gibart, "III nitrides and UV detection", *J. Phys.: Condens. Matter.*, vol. 13, pp. 7115-7137, 2001.
- [5]. M. Razeghi and A. Rogalski, "Semiconductor ultraviolet detectors", *J. Appl. Phys.*, vol. 79, pp. 7433-7473, 1996.
- [6]. A. Ionascut-Nedelcescu, C. Carlone, A. Houdayer, H.J. von Bardeleben, J.-L. Cantin, and S. Raymond, "Radiation hardness of gallium nitride", *IEEE Trans. Nucl. Sci.*, vol. 49, pp. 2733-2738, 2002.
- [7]. D. Walker, V. Kumar, K. Mi, P. Sandvik, P. Kung, X.H. Zhang, and M. Razeghi, "Solar-blind AlGaIn photodiodes with very low cutoff wavelength", *Appl. Phys. Lett.*, vol. 76, pp. 403-405, 2000.
- [8]. B.W. Lim, Q.C. Chen, J.Y. Yang, and M. Asif Khan, "High responsivity intrinsic photoconductors based on Al_xGa_{1-x}N", *Appl. Phys. Lett.*, vol. 68, pp. 3761-3762, 1996.
- [9]. G.A. Shaw, A.M. Siegel, and J. Model, "Ultraviolet comm link for distributed sensor systems", *IEEE LEOS Newslett.*, vol. 19, pp. 26- 29, 2005.
- [10]. J. Schalwig, G. Müller, O. Ambacher, and M. Stutzmann, "Group III-nitride-based sensors for combustion monitoring", *Mater. Sci. Eng. B*, vol. 93, pp. 207-214, 2002.
- [11]. A. Rogalski and M. Razeghi, "Semiconductor ultraviolet photodetectors", *Opto-Electron. Rev.*, vol. 4, pp. 13-30, 1996.
- [12]. J. Wu, W. Walukiewicz, K.M. Yu, W. Shan, J.M. Ager III, E.E. Haller, H. Lu, W.J. Schaff, W.K. Metzger, and S. Kurtz, "Superior radiation resistance of In_{1-x}Ga_xN alloys: full-solar-spectrum photovoltaic material system", *J. Appl. Phys.*, vol. 94, pp. 6477-6482, 2003.
- [13]. O. Jani, I. Ferguson, C. Honsberg, and S. Kurtz, "Design and characterization of GaN/InGaIn solar cells", *Appl. Phys. Lett.*, vol. 91, p. 132117, 2007.
- [14]. P. Hohenberg and W. John, *Phys. Rev.* 136, B 864 (1964)
- [15]. W. Kohn and L. J. Sham, *Phys. Rev.* 140, A1133 91965)
- [16]. X. Gonze, G.-M. Rignanese, M. Verstraete, J.-M. Beuken, Y. Pouillon, R. Caracas, F. Jollet, M. Torrent, G. Zerah, M. Mikami, Ph. Ghosez, M. Veithen., J.-Y. Raty, V. Olevano, F. Bruneval, L. Reining, R. Godby, G. Onida, D. R.Hamann, and D. C. Allan. (2005). A brief Introduction to the Abinit software package. *Z. Kristallogr.* 220, 558-562.
- [17]. X. Gonze, J.-M. Beuken, R. Caracas, F. Detraux, M. Fuchs, G. M. Rignanese, L. Sindic, M. Verstraete, G. Zerah, F. Jollet, M. Torrent, A. Roy, M. Mikami, Ph. Ghosez, J.Y. Raty, and D.C. Allan (2002). *Computational Materials Science* 25, 478-492.

- [18]. M. Fuchs and M. Scheffler (1999). Ab initio pseudopotential for electronic structure calculations of poly-atomic systems using density functional theory. *Comput. Phys. Commun.* 119, 67- 72.
- [19]. S. Y. Savrasov, (1996). Linear-response theory and lattice dynamics: A muffin-tin-orbital approach. *Phys. Rev. B* 54, 16470–16486.
- [20]. D. Marel, van der and Sawatzky, (1988); Electron-electron interaction and localization in *d* and *f* transition metals. *Phys. Rev. B* 37, 10674–10684.
- [21]. S. Goedecker, M. Teter, and J. Hutter, *Phys. Rev. B*, 54, 1703 (1996).
- [22]. M. Teter, *Phys. Rev. B*, 48, 5031 (1993).
- [23]. J. P. Perdew, K. Burke, and M. Ernzerhof, *Phys. Rev. Lett.*, 77, 3865 (1996).
- [24]. H. Y. S. Shalash (2009). FP-LAPW Study Of Phase Changes In An (A=Al,In, and B) Under High Pressure. Degree of Master of Science in Physics, An-Najah National University, Nablus, Palestine.
- [25]. K. M. Benail (2004). First principle study of structural, elastic and electronic properties of AlN and GaN semiconductors under pressure effect and magnetism of AlN: Mn and GaN: Mn systems. Doctor's Thesis. Abou-Bakr Belkaid University-Tlemcen, Algeria .
- [27]. Zhao G. L., Bagayoko D., and Williams T. D. (1999). Local-density-approximation prediction of electronic properties of GaN, Si, C and RuO₂ . *Phys. Rev. B* 60, 1563-1572.
- [28]. I. Vurgaftman. and J.R. Meyer (2003). Band parameters for nitrogen-containing semiconductors. *J. Appl. Phys.* 94, 3675 -3697.
- [29]. G. Ramirez-Flores, H. Navarro-Contreras, A. Lastras-Martinez, R. C. Powell and J. E. Greene (1994). Temperature-dependent optical band gap of the metastable zinc-blende structure β -GaN. *Phys. Rev. B* 50, 8433-8438.
- [30]. B. D. F. Zpeedeh (2008). First Principle Electronic Structure Calculations of Ternary alloys. BN_xP_{1-x} and Ga_xB_{1-x}N in zinc blende structure. Master of Science in physics An-Najah National University, Nablus –Palestine.
- [31]. L. E Ramos, L. K Teles, L.M.R Scolfaro, J.L.P Castineira, A. L Rosa, J.R Leite (2001). Structural, electronic, and effective-mass properties of silicon and zinc-blende group-III nitride semiconductor compounds. *Phys. Rev. B* 63, 165210-165219.
- [32]. I. Petrov, E. Mojab, P. C. Powell, J. E. Greene, L. Hultman and J. E. Sundgren (1992). Synthesis of metastable epitaxial zincblende structure AlN by solid state reaction. *J. Applied Physic. Lett.* 60, 2491.
- [33]. V. Cimalla, J. Pezoldt, G. Ecke, R. Kosiba, O. Ambacher, L. Spie, H. Lu, W. J. Schaff, and G. Teichert (2003). Growth of cubic InN on r-plane sapphire. *J. Applied Physics. Lett.* 83, 3468 - 3471.
- [34]. Y. N. Xu and W. Y. Ching (1993). Electronic, optical and structural properties of some wurtzite crystals. *Phys. Rev. B* 48, 4335-4351.
- [35]. G. L. Zhao, D. Bagayoko and T. D. Williams (1999). Local-density-approximation prediction of electronic properties of GaN, Si, C and RuO₂ . *Phys. Rev. B* 60, 1563-1572.
- [36]. A. Zaoui and F. El-Haj Hassan (2001). Full potential linearized augmented plane wave calculations of structural and electronic properties of BN, BP, BAs and BSb. *J. Phys. Condens. Matter* 13, 253-262.
- [37]. B. Daoudi, M. Sehill, Boukraa A. and Abid H. (2008). FP-LAPW calculations of ground state properties for AlN, GaN and InN compounds. *Int. J. Nanoelectronics and Materials.* 1, 65-79.
- [38]. Edgar J.H. (1994). Properties of group III nitrides. Institution of Electrical Engineers, London, UK.
- [39]. Onodera A., Nakatani M., Kobayashi M., Nisida Y. (1993). Pressure dependence of the optical-absorption edge of cubic boron nitride. *Phys. Rev. B* 48, 2777–2780.
- [40]. Marques M, Teles L. K., Scolfaro L. M. R., Leite J. R., Furthmüller J, and Bechstedt F. (2003). Lattice parameter and energy band gap of cubic Al_xGa_yIn_{1-x-y}N quaternary alloys. *Appl. Phys. Lett.* 83, 890-892